

Therapeutic oligonucleotide (nusinersen) metabolism in cerebrospinal fluid samples of patients with spinal muscular atrophy based on liquid chromatography coupled with mass spectrometry data

Sylwia Studzińska^{a,b,*}, Anna Lemska^c, Jakub Szymarek^c, Maria Mazurkiewicz-Beldzińska^c

^a Chair of Environmental Chemistry and Bioanalytics, Faculty of Chemistry, Nicolaus Copernicus University in Toruń, 7 Gagarin Str., PL-87-100 Toruń, Poland

^b Institute of Advanced Studies, Nicolaus Copernicus University in Toruń, 4 Wilenska Str., PL-87-100 Toruń, Poland

^c Department of Developmental Neurology, Medical University of Gdansk, 7 Dębinki Str., PL-80-952, Gdańsk, Poland

*Corresponding author: kowalska@umk.pl

Abstract

Background: Spinal muscular atrophy (SMA) is a severe genetic neuromuscular disorder caused by a deficiency of the survival motor neuron protein. The introduction of antisense oligonucleotide therapy has markedly improved prognosis, particularly following approval of Nusinersen (Spinraza), the first SMA drug. Although modified with 2'-O-methoxyethyl and phosphorothioate groups, nusinersen is metabolized. Comprehensive characterization of these metabolites in cerebrospinal fluid is limited due to analytical challenges associated with antisense oligonucleotides. This study aimed to develop a first liquid-liquid/solid-phase extraction procedure combined with ion-pair ultra-high-performance liquid chromatography coupled with mass spectrometry for the extraction, separation, and identification of nusinersen and its metabolites in cerebrospinal fluid samples from SMA patients treated with Spinraza.

Results: A two-step sample preparation procedure provided high nusinersen recovery (89.2±1.8%), repeatability, eliminated matrix effects, and enabled 50-fold sample concentration. All of these proved essential for the detection and identification of low-abundance metabolites collected four months after dosing. Reliable metabolite identification requires sufficient chromatographic resolution, especially for metabolites differing by a single nucleotide with similar nominal m/z values. Consequently, careful ion-pair reagent selection and MS optimization are crucial for improving separation and sensitivity to detect low-abundance metabolites. Our results showed that propylamine and dimethylbutylamine may be used interchangeably, but the second one provides higher resolution. Accurate mass measurement and characteristic fragment ions derived from methylated nucleobases and phosphorothioate groups ensured reliable identification. Analysis of CSF samples from 17 pediatric SMA (at various dosing stages) patients revealed extensive in vivo metabolism, predominantly via 3'-exonucleolytic cleavage, yielding multiple N-shortmers. For the first time, interpatient variability was observed in nusinersen detectability and metabolite profiles of CSF samples.

Significance: To our knowledge, this is one of the first comprehensive studies demonstrating the applicability of the developed procedure to observe differences in the metabolism of nusinersen and, in the future, linking them to therapeutic effects, therapeutic monitoring, or the patient's condition. The methodology addresses key bioanalytical challenges

(reproducibility, purification, concentration, separation) and enables metabolite profiling in a complex biological matrix. Moreover, it provides a foundation for future investigations linking metabolism, drug exposure, and clinical response in SMA therapy.

Keywords: nusinersen; metabolites; extraction; ion pair ultra high liquid chromatography coupled with mass spectrometry; cerebrospinal fluid; therapeutic effect; spinal muscular atrophy

1. Introduction

Spinal muscular atrophy (SMA) is a rare genetic disease caused by a deficiency of the survival motor neuron (SMN) protein, most commonly due to a mutation of the SMN1 gene [1,2]. Until 2016, it was a fatal disease due to the weakness or atrophy of muscles (ongoing problems with moving, swallowing, breathing). The introduction of antisense oligonucleotide (ASO) therapy has significantly changed the prognosis for patients [2]. Nusinersen, an active ingredient in Spinraza, was the first approved disease-modifying treatment for SMA and is now widely used in pediatric and adult patients [1–3]. Nusinersen is a fully modified 2'-O-methoxyethyl phosphorothioate oligonucleotide (ON) designed to increase the effectiveness of SMN biosynthesis [1,4,5]. Structural modifications introduced within the ribose moiety, phosphate backbone, and pyrimidine bases significantly decrease nuclease degradation and prolong biological activity [6]. However, despite its stability, nusinersen undergoes *in vivo* metabolism, primarily through exonucleolytic cleavage from the 3' end, leading to the formation of truncated metabolites (N-shortmers) [6,7]. Understanding the metabolic fate of nusinersen in cerebrospinal fluid (since a lumbar puncture is used to administer Spinraza) is essential for comprehensive pharmacokinetic characterization and may provide insights into interpatient variability in therapeutic response. Therefore, the development of methods useful for the analysis of nusinersen metabolites is important [3,5,8]. Nevertheless, bioanalysis of ASO remains challenging from an analytical perspective due to its high polarity, tendency toward nonspecific adsorption, and low concentrations encountered in biological matrices [9–11].

To date, some studies have focused on quantifying nusinersen concentrations in serum and CSF using hybridization-based immunoassays (e.g., hybridisation nuclease enzyme-linked immunosorbent assay, ELISA) or electrochemiluminescence methods [1]. While these techniques offer high sensitivity, they do not provide structural information and are therefore unsuitable for metabolite identification. In contrast, liquid chromatography coupled with mass spectrometry (LC-MS) enables simultaneous detection and structural characterization of ASO and their metabolites [[9,10]. It was used for the analysis of the proteome in CSF after administering nusinersen [12] or for the determination of nusinersen itself in the plasma of CSF samples [3,5,7,8]. Ion pair high performance (IP RP HPLC) coupled with MS provides optimal retention with high sensitivity (lower limit of quantification in the range of 2-5 ng mL⁻¹), linearity, and precision [3–5]. The problems reported so far in the nusinersen analytics are the selection of internal standard (high price of isotope-labeled one, application of homooligonucleotides e.g., dT20) [3,5] and carryover (reduced by elevated column temperature, high flow rate flushing, multiple gradient cycles, increase mobile phase pH) [5,8].

Even though IP RP UHPLC MS has emerged as a powerful platform for ASO analysis, hydrophilic interaction liquid chromatography was also used [8]. An undeniable advantage was the lack of ion pair reagents, but sensitivity was lower (30 ng mL^{-1}) compared to IP RP UHPLC. Moreover, the non-specific nusinersen adsorption was noticed when the pH of the mobile phase was lowered below 4 [8]. Another limitation was column blockage observed when the pH value of the mobile phase was at a lower level, especially at high concentrations of nusinersen. Another interesting approach was the application of magnetic nanoparticles modified with single-strand binding protein with selective bonding of red fluorescent quantum dots functionalized with ONs [13]. The procedure showed very high specificity and sensitivity for nusinersen (limit of detection = 0.03 nM), but not for its metabolites [13].

Nusinersen was extracted from plasma or CSF (rats, rabbits) using two methods so far. First one involved protein precipitation using 0.01% triethylamine in MeOH or ACN, which is not a routine practice for ASO [5]. However, no information on recovery or matrix effect was provided for this approach. Solid phase extraction (SPE) is more commonly used for ASO extraction [3,8]. Two different SPE cartridges were applied during nusinersen extraction from plasma and CSF: Clarity® OTX and Oasis HLB. The first one provided a recovery of 93-96%, while the second one provided only 67-75% [4,8].

Although several studies have addressed nusinersen quantification in plasma or CSF, reports describing comprehensive extraction, chromatographic separation, and identification of nusinersen metabolites in CSF samples from SMA patients remain scarce [14]. There are several reports on nusinersen metabolites in plasma [7,15], but more publications focus on the modulation of gene expression [[16], changes in the biochemical components (glucose, protein) in the CSF [17], and multi-proteomic CSF analysis dependent on nusinersen treatment [18]. Moreover, some small-molecule metabolites were identified as predictive of nusinersen efficacy (e.g. 1-acryloyl-2-hydroxy-sn-glycero-3-phosphate, N-myristoyl arginine, 1,1,1,2,2-pentafluoro-7-phenylheptan-3-one) [19] The present study aimed to develop a robust LLE/SPE IP-RP-UHPLC-Q-TOF-MS workflow for the extraction, separation, and identification of nusinersen and its metabolites in CSF samples from patients with SMA treated with Spinraza. Special emphasis was placed on optimization of chromatographic and MS conditions, and reliable differentiation of truncated metabolites. By applying this approach to clinical samples, we sought to characterize nusinersen metabolic profiles in vivo and to explore the potential of the developed procedure as a tool for improved understanding of therapeutic oligonucleotide metabolism in the central nervous system. To the best of our knowledge, this is one of the first studies of this kind.

2. Materials and methods

2.1. Materials and methods

The LC-MS grade water, N-hexylamine (HA), N,N-dimethylbutylamine (DMBA), N-propylamine (PA), N,N-diethylamine (DEA), N,N-diisopropylethylamine (DIPEA), 1,1,1,3,3,3-hexafluoroisopropanol (HFIP) were purchased from Merck (Warsaw, Poland). The LC-MS grade methanol (MeOH) was purchased from Honeywell. Deionized water was obtained from a Milli-Q system (Millipore, El Paso, USA). The mixture of phenol/chloroform/isoamyl alcohol (25:24:1) (saturated with 10 mM Tris, pH 8.0, 1 mM EDTA) (Merck, Warsaw, Poland) was also used.

The SupelTM Swift HLB SPE cartridges were purchased from Merck (Warsaw, Poland) and used during the extraction. The chromatographic analysis was performed using the Acquity Premier Oligonucleotide BEH C18 (1.7 μm , 130 \AA , 2.1 \times 100 mm) (Waters, Massachusetts, US) column with a pre-column.

Nusinersen has the following sequence 3'-mU*mC*A*mC*mU*mU*mU*mC*A*mU*A*A*mU*G*mC*mU*G*G-5', where 'm' denotes an additional methyl group in cytosine and uracil, * stands for a phosphorothioate group. Each ribose molecule in nusinersen's structure possesses a 2'-O-methoxyethoxyl group. The molecular mass of nusinersen equals 7127 g/mol. The standard of this compound was purchased in Future Synthesis (Poznań, Poland) in lyophilized form (synthesis scale 0.2 μM) and dissolved to a concentration of 100 μM (using deionized water). It was purified in two steps, namely RP HPLC and ion-exchange chromatography.

2.2. Instruments

The SPE Vacuum Manifold CHROMABOND (12 positions) was purchased from Macherey-Nagel (AnchemPlus, Warsaw, Poland) and used during the study. This study employed a 1260 Infinity Quaternary UHPLC system (Agilent, Waldbronn, Germany) coupled to an Agilent 6540 UHD Accurate-Mass Quadrupole Time-of-Flight mass spectrometer (Waldbronn, Germany). Nusinersen and its metabolites were analyzed using electrospray ionization (Q-TOF-MS) in negative ion mode. Full-scan mass spectra were acquired over an m/z range of 500–3200, while fragmentation spectra were recorded across m/z 50–1000 for collision energies between 10 and 200eV (every 10eV). Data acquisition was performed simultaneously in centroid and profile mode using Agilent MassHunter software (version B.04.01).

During extraction, samples were centrifuged using a Frontier Micro FC5515 centrifuge from OHAUS Europe GmbH (Nänikon, Switzerland). The glass SPE vacuum chamber 12G (Baker, Witko, Łódź, Poland) was also used during the extraction. Graphs and chromatograms included in the paper were prepared using OriginPro2025 (OriginLab Corporation, Northampton, MA, USA).

2.3. CSF samples

The other oligonucleotide used during the study, namely OL1 (sequence 5'-GGTCGTAATACTTTCAT-3'), was purchased from Merck (Gillingham, Dorset, UK) and used for saturation. The stock concentration of OL1 was 0.1 mM.

The samples were taken following the relevant guidelines of the Medical University of Gdańsk and approved by the Independent Bioethics Committee for Scientific Research at the Medical University of Gdańsk (permission no. NKBBN/778/2022). A total of 17 pediatric patients were participants in the study. They were children with genetically confirmed SMA aged from 3 to 16 years old. They differed in age, body weight, SMA type, and health status. We have compiled basic information about the patients in Table S1. The children were enrolled at the Division of Developmental Neurology, the Medical University of Gdansk, at the University Clinical Centre, with the consent of the parents, providing full information about the examination. CSF was collected during Spinraza administration. An initial 5 mL of CSF was withdrawn, followed by the intrathecal administration of 5 mL of the Spinraza solution. As the samples were taken during drug administration, each of them was actually collected 4 months after the previous dose of Spinraza (from the third month of therapy, this drug is administered every 4 months).

2.4. Extraction of nusinersen and its metabolites

CSF samples were immediately frozen and stored at -20 °C until analysis (from 2 weeks to 3 months). Next, upon thawing, they were processed according to the procedure outlined in the subsequent sections. Samples were kept on ice before liquid-liquid extraction (LLE). The sample preparation was based on a previously developed procedure published by our team [[14]. The 5 mL of CSF was divided into two samples (2.5 mL each). Next, LLE using a 2.5 mL phenol/chloroform/isoamyl alcohol mixture (25:24:1 v/v) was performed. The suspension was mixed and centrifuged (RCF 20160×g for 40 minutes). The supernatant was transferred to another Falcon tube, and an additional LLE extraction step was performed to remove residual phenol (significantly reducing ionization in MS). Chloroform was used at a 4:1 (chloroform:

extract) ratio. Next, SPE was applied to further purify and concentrate the sample. The Swift HLB SPE cartridges were applied (30 mg, 1 mL). The following solvents were used during the conditioning: 1 mL acetonitrile, 1 mL water, 3 mL 5mM N-hexylamine (HA)/150mM 1,1,1,3,3,3-hexafluoroisopropanol (HFIP). The LLE extract was mixed with 5mM HA/150mM HFIP in a ratio of 1:1, and then loaded onto the surface of the SPE cartridge. The cartridge was washed with 500 μ L of 90/10% v/v 5 mM DMBA/150 mM HFIP/MeOH. The nusinersen and its metabolites were eluted using 1 mL of 10/90% v/v 5mM DMBA/150mM HFIP/MeOH. The vacuum was used during the conditioning and washing of the SPE cartridges, while gravity flow was applied for sample load and elution. This is a result of using ion-pair mode during SPE extraction. The dynamically formed anion-exchange centers require more time to adsorb ONs and efficiently desorb them; consequently, gravity flow is usually used [15,20,21]. The use of gravity flow ensures complete adsorption and complete desorption. SPE extracts were evaporated to dryness at 40 °C, and the residue was dissolved in 50 μ L of mobile phase. The sample volume was reduced from 2.5 mL to 50 μ L, consequently 50-fold concentration was achieved.

The sample preparation procedure was first tested against blank CSF samples fortified with nusinersen to a final concentration of 0.05 μ M. Recovery, repeatability, and matrix effect (ME) were calculated for LLE and LLE-SPE using fortified CSF samples. The limit of detection (LOD) and quantification (LOQ) were determined experimentally using the signal-to-noise ratio method. The first one is the concentration at which the signal-to-noise ratio is at least 3:1, while LOQ is the concentration at which the signal-to-noise ratio is at least 9:1.

The ME was determined during the study for nusinersen standard. Initially, 2.5 mL of a CSF sample was subjected to the extraction procedure (LLE and SPE, respectively) without the addition of nusinersen standard, yielding a blank matrix extract. Subsequently, the blank extract was fortified with a nusinersen to achieve a final concentration of 0.05 μ M. Chromatographic analysis was then carried out for both the standard and the spiked blank extract (at the same nominal concentration of 0.05 μ M). The peak areas obtained from the post-extraction spiked matrix were compared with those of the neat standard solution at an equivalent concentration. The following equation was applied:

$$ME = \frac{A1}{A2} * 100\%$$

where: ME – matrix effect; A1 – peak area of nusinersen in post-extraction spiked matrix; A2 – peak area of nusinersen standard.

2.5. LC-MS conditions

The optimized gradient elution was performed using 26-44% v/v MeOH over 15 min at a mobile phase flow rate of 0.3 mL min⁻¹. Next, MeOH was kept at 44% v/v for 1 minute and reduced over the next minute to 26% v/v. The injection volume was 2.5 μL. The autosampler was maintained at 4 °C, and the column temperature was set to 60 °C. The Q-TOF-MS operating conditions for nusinersen standard were optimized by design of experiments using Box-Behnken design. Three sets of independent variables were tested: 1. drying gas temperature (DGT, 60–360 °C), shielding gas temperature (SGT, 60–360 °C), octopole voltage (OV, 40-800V), 2. nebulizer gas pressure (NGP, 15-80 psig), drying gas flow (DGF, 2-10 L min⁻¹), shielding gas flow (SGF, 8-12 L min⁻¹), 3. skimmer voltage (SV, 10-350 V), capillary voltage (CV, 500-6000 V), fragmentor voltage (FV, 10-300 V). The peak areas at extracted ion chromatogram (EIC) for m/z = 2374.420 (nusinersen standard) were dependent variables. Thirteen chromatographic analyses were performed (in replicates) in each case under a developed chromatographic method. The values of parameters of the Box-Behnken design were calculated using the online statistics calculator Numiqo e.U [22]. The range of the tested values and EIC peak areas is collected in Table S2. Based on the obtained results, 2D contour plots were prepared using the Statistica package (StatSoft Inc, Tulsa, USA). Collision energy was also optimized by analysis of nusinersen standard, though systematically changing the energy by 10 eV in the range of 20-180 eV and recording fragmentation spectra. It should be noted that the reported collision energies correspond to singly charged ions; thus, for multiply charged oligonucleotide ions, the effective collision energy equals the applied collision voltage multiplied by the ion charge.

During the study of the effect of amines on the MS detector response (peak area at EIC, ions at the full scan spectra), isocratic elution was used, and the whole study was carried out without the column. The composition of the mobile phase was as follows: 1. for the study of the effect of the type of amine: 50/50% v/v 5mM amine with 150 mM HFIP/MeOH; 2. for the study of the effect of methanol: 5mM DMBA with 150 mM HFIP with 10, 35, 60, 85 % v/v MeOH. The other conditions (MS, column, and autosampler temperatures, flow rate) remained unchanged.

3. Results and discussion

The development of a robust method for the extraction, separation, and identification of nusinersen metabolites in cerebrospinal fluid (CSF) samples of children with SMA is necessary for several interrelated pharmacological, bioanalytical, and medical reasons. Without

metabolite-specific analytical tools, it is impossible to fully characterize the metabolism of this ON in the central nervous system. It is essential for accurate pharmacokinetic and pharmacodynamic interpretation, as well as a clinical perspective. While several studies have described quantification of nusinersen in biological samples, none of them have demonstrated successful analysis of its metabolites in CSF. Establishing such a method will expand the bioanalytical toolbox for therapeutic ONs and provide a base for studies exploring the relationship between metabolism and clinical outcome. To the best of our knowledge, this is the first study of this kind presenting a comprehensive procedure for nusinersen metabolites in samples collected from 17 patients with SMA treated with Spinraza.

3.1. Nusinersen stability

In the initial stage, the stability of nusinersen against degradation was tested depending on the number of thawing and freezing cycles. Nusinersen was dissolved in water and frozen at -20 °C. It was then thawed monthly for a period of 5 months. IP RP UHPLC Q-TOF-MS analyses did not show any degradation of the compound. An aqueous solution of nusinersen was also stored at 4 °C for a month, with no degradation observed after 2 weeks (Table S3). An aqueous solution of this compound was also stored at room temperature for 24 hours, and in this case, no degradation was observed either (Table S3). Significant modifications introduced in the structure of nusinersen (ribose, phosphate group, and pyrimidine nitrogen bases) increase its stability during freezing/thawing. This makes it possible to work with this compound without the risk of its rapid degradation.

The stability of nusinersen was also tested in LLE and SPE extracts. For this purpose, the extracts were stored at 4 °C for 24 hours, and nusinersen remained stable (Table S3). A similar situation was noticed when extracts were stored at room temperature for 2 hours. Next, the collected extracts, both after LLE and SPE, were frozen at -20 °C, then thawed after two and four months and analyzed using IP RP UHPLC Q-TOF-MS (Table S3). Nusinersen was stable and did not degrade over this period after freezing/thawing. This information is important for routine laboratory work on CSF sample preparation. The extracts did not need to be stored on ice and could be reanalyzed after several months without losing the reliability of the data obtained.

3.2. LC-MS method

3.2.1. Saturation

Scientific literature provides extensive information on the analysis of antisense oligonucleotides using liquid chromatography coupled with mass spectrometry (LC-MS). One of the most important findings in the routine analysis of these compounds is their non-specific adsorption on the steel surfaces of LC-MS systems [23–25]. UHPLC Q-TOF-MS used during our investigations was non-bioinert, contrary to the column used. Before analyzing the nusinersen standard or CSF extracts, we saturated the entire system using the unmodified oligonucleotide standard OL1 (5 injections of 5 μ L at 100 μ M) while monitoring the detector response (EIC peak area) on the chromatogram. This was sufficient to obtain a stable quantitative response. We then performed 3 control injections of the nusinersen standard (5 μ L of standard at a concentration of 10 μ M) to ensure that the peak area was stable between injections.

3.2.2. Nusinersen mass spectra

The full scan and deconvoluted mass spectra of nusinersen are presented in Figure 1A and B. The electrospray ionization produces a series of multiply charged ions, and the resulting mass spectrum displays a characteristic charge-state envelope. The observed signals are due to the presence of negatively charged phosphorothioate groups along the nusinersen backbone. Nusinersen mass spectra show broad charge state distribution from $z=-3$ to $z=-8$, as is characteristic for ONs analyzed under denaturing conditions, such as high column temperature (60 $^{\circ}$ C in our case), when unfolded, linear structure is dominant (contrary to possible hairpin forms present at low temperature with fewer ions observed at mass spectra), resulting from the availability of a greater number of phosphate groups for deprotonation [26,27]. Typically, ion intensities vary significantly with charge state due to differences in ionization efficiency and gas-phase stability. Intermediate charge states usually exhibit the highest intensities, while very low and very high charge states are less abundant [28–31]. However, nusinersen mass spectra show a different pattern of ion intensity distribution, since intermediate charge states (-4, -5) are the lowest. The highest intensities were observed for $m/z=1017.035$ ($z=-7$) and $m/z=2374.420$ ($z=-3$), with the latter being the highest (Figure 1A). The typical spectrum of nusinersen recorded to date and presented in scientific literature covers a m/z of 700-1800, with $m/z=1017.035$ having the highest intensity [5,8,27]. In initial trials, we also worked in the m/z range up to 1700. Increasing the m/z range to 500-3200 led to an increase in the range of ions observed in the spectra, which proved to be advantageous because the $m/z=2474.420$ ion has greater intensity, which increases sensitivity.

Regarding the charge states intensities at the full scan spectra, higher and lower charge states are apparently efficiently formed during nusinersen electrospray ionization (-3 and -7) (Figure 1A). It may result from mobile phase composition, as suggested in the literature [32,33] and shown in our study. Data collected in Table S4 presents the impact of amine type and MeOH content in the mobile phase on the full scan mass spectra of nusinersen. The use of HA or DMBA changes the distribution of charge state intensities, with $m/z = 1780.562$ and $m/z = 2374.420$ being the most intense, respectively. A change in the percentage of MeOH can also lead to a change in the intensity of signals in the spectrum (Table S4). Furthermore, during the optimization of ion source parameters in MS (described below), we noticed that charge state distribution (the intensities of ions with different charges) varies depending on the conditions. This effect was observed only when gas temperatures were changed and concerned only two ions with $z=3$ (2374.420) and $z=7$ (1017.035). When DGT was lower than 100 °C, $m/z=1017.035$ was the most abundant ion, while $m/z=2374.420$ was the highest for other higher temperatures. The resulting intensity distribution reflects an equilibrium between desolvation efficiency in the ion source, molecular conformation of nusinersen, and charge accommodation capacity. To conclude, the charge-state distribution and intensities observed in nusinersen mass spectra result from the mobile phase composition and MS parameters. Results confirm the need to monitor spectra at given experimental conditions, especially for monitoring of ON metabolites, where the sensitivity is the key parameter, since their concentration is lower. Moreover, the application of a wider m/z range for mass spectra is beneficial as it allows a more appropriate selection of the parent ion and consequently increases sensitivity and specificity (as it will be shown in the following sections).

Finally, $m/z=2374.420$ and $m/z=1017.035$ ions were selected for monitoring of the peak areas at EIC during optimization of MS parameters, fragmentation, or extraction.

3.2.3. Nusinersen fragmentation

The fragmentation of nusinersen provides additional structural information through backbone fragmentation, enabling the distinction of which signals on the spectra originate from nusinersen or its derivatives. This approach may appear as an essential tool for verifying the identity of nusinersen metabolites.

The effect of changes in collision energy on the fragmentation of nusinersen was tested across the entire range from 10 to 200 eV. Figure 1 C, D, and E show exemplary spectra recorded for 10, 100, and 190 eV. For low collision energies, signals originating from 5-methyluracil ($m/z=125.0350$), adenine ($m/z=134.0469$), and the phosphorothioate group

($m/z=94.9359$) were recorded, as well as signals from monophosphorothioate nucleotides (with ribose modified with 2'-O-methoxyethoxyl group), namely 5-methylcytidine ($m/z=393.0521$), adenosine ($m/z=402.0632$), and guanosine ($m/z=418.0584$) (Figure 1C). Increasing the collision energy (from 10 to 100eV) results in further bond cleavage; consequently fragmentation spectrum exhibits characteristic phosphate and nucleobase fragment ions typical of ON fragmentation (Figure 1D). Nucleotides fragment ions disappear, while signals originating from 5-methyluracil, adenine, and POS^- (78.9588), PO_2S^- (94.9359), and PO_3S^- (134.0468) groups are more intense (Figure 1 D). Further increasing the collision energy (from 110 to 200eV) leads to rapid degradation as only three fragment ions originating from the phosphorothioate group and 5-methyluracil remain (Figure 1E). The spectra show strong nucleobase-derived ions, consistent with the known preference of ONs to undergo cleavage of the glycosidic bond before backbone degradation. A change in collision energy causes not only a change in fragment ions, but also a change in their intensity. In the case of our study, 100eV was selected for nusinersen metabolites monitoring, since it provided fragmentation spectra with characteristic signals of high intensity (Figure 1D).

Due to the modification of nucleobases and phosphate group in nusinersen structure, one of the base-derived fragment ions (5-methyluracil) is characteristic for this compound, similarly to the phosphorothioate group. These are $m/z=94.935$ and $m/z=125.0351$ (Figure 1D, E). We selected both of them for additional confirmation during metabolite identification. None of the other compounds present in cerebrospinal fluid (e.g., nucleic acids, proteins, lipids) will be fragmented with the production of analogous fragmentation ions, as in the case of nusinersen or its metabolites, because the ions we have selected are closely related to modifications of this compound (specific ones). This is another bioanalytical advantage, in addition to the high stability of modified therapeutic nusinersen (as indicated in the previous section). Sequence-specific fragment ions allow rapid and efficient confirmation of nusinersen and its metabolites presence in the sample.

3.2.4. Metabolites identification

Several approaches were applied for the characterization and identification of metabolites. The first one involved simple monitoring of EICs (for specific m/z values of a precursor ion at a certain charge state) from the predicted molecular formulas, as it is the most commonly used method [7,28,30]. We have calculated a predictive list of m/z values (Table S5) for potential metabolites. We did not use any software to calculate potential metabolites because nusinersen has three different modifications in its structure. There is currently no online

analytical tool available to calculate the masses of this type of metabolite (with three different modifications). We prepared an Excel file in which, by creating sequences (based on the structure), the molecular formula was calculated, and consequently, the masses of individual compounds, as well as the corresponding m/z values for individual ions, were determined (Table S5). We focused on two possible metabolism pathways of nusinersen: shortening of the sequence by successive nucleotide cleavage from the 3' or 5' ends (N-shortmers) (noted as e.g., 3'N-3, 5'N-2) (Table S5). The truncated metabolites were the ones mainly observed for therapeutic ONs so far in the literature [28,30,34]. We calculated molecular mass, formula, m/z for metabolites with a nucleotide cleavage at the 3' and 5' ends, and the same metabolites with an additional PO_3^- group (noted as e.g. 3'N-3PS, 5'N-2PS) at the 3' and 5' ends (Table S5). Using a good-quality separation method, metabolite identification can be performed readily, but we have also used deconvoluted masses for additional confirmation. The high resolution of Q-TOF-MS allowed the identification of metabolites from the measured accurate masses. Moreover, as described in the former section, fragmentation of selected ions was applied for supplementary confirmation that the signals identified as metabolites are derivatives of nusinersen (based on characteristic fragment ions originating from methylated uracil and the phosphorotioate group). This is particularly important in the case of extraction, where, in addition to ONs, there is a risk of isolating other polar compounds that can produce multiply charged signals in the mass spectrum (in the case of CSF, we believe these may be proteins, sugars, or possibly lipids).

3.2.5. *Mobile phase impact*

Based on our previous experience in ASO analysis, ion-pair chromatography was selected for the study of nusinersen and extracts from cerebrospinal fluid samples [7,10,15,30]. This chromatographic mode has so far provided the highest possible resolution of ASOs. The primary objective of our study was to achieve a good separation of nusinersen metabolites and their subsequent identification. A chromatographic column with an octadecyl stationary phase was selected because it had proven useful in previous studies for separating mixtures of modified therapeutic oligonucleotides. We did not test other columns in this experiment, but decided to focus our attention on the selection of the mobile phase composition by the change made in the amine. In each case, HFIP was simultaneously added to the mobile phase, increasing the volatility of the mobile phase (boiling point 49 °C) and consequently ionization of ONs [29]. HFIP is beneficial for ASO analysis for several other reasons, e.g. provide amine

protonation, maintains reproducible retention, lowers pH of the mobile phases (extends column lifetime), improves retention and MS sensitivity [35–37].

Even though there are already many reports and comprehensive studies in scientific literature on the influence of various amines on ON retention or the intensity of their signals in MS [28,31,35,37–40], we conducted such studies for nusinersen because we are convinced that it is highly necessary to test the compatibility of target ON with a specific ion-pair reagent. This belief stems both from our experience and from data presented in the literature [34]. The following amines were tested, namely, PA, DEA, HA, DMBA, and DIPEA. Their concentration was equal to 5mM, while the concentration of HFIP was kept constant at 150mM. The peak areas at EIC for nusinersen standard were monitored, and the results were collected in Table 1. Differences were observed depending on the amine used, since several amine features have an impact on the sensitivity of therapeutic ONs analysis by IP RP UHPLC MS. These are e.g., boiling point, pKa, Henry's law constant (parameters collected in Table 1) [35,41]. The pKa values are similar for all tested amines and therefore cannot be considered as critical or differentiating ones. The ONs ionization efficiency should typically be higher when an amine with a high volatility and a high Henry's law constant is used, because these parameters impact evaporation from the droplet as nusinersen is ionized. This remains true for two of the tested amines, PA and DEA, where the highest EIC peak areas were obtained (Table 1). Application of HA with a high boiling point and low Henry's law constant resulted in low MS detector response for nusinersen, which seems to confirm the influence of both parameters on ionization efficiency. On the other hand, the use of DIPEA, with a low Henry's law constant and a high boiling point, yielded only a 7% lower peak area. Some of the literature suggests that amine structure impacts sensitivity by lowering the detector response for primary amines [35]. In the case of nusinersen study, the opposite effect for two primary amines (PA and HA) was noticed. Moreover, similar results for primary and secondary amines (PA and DEA) were observed. Consequently, our results do not fully confirm all of the tendencies suggested so far in the literature [35,41]. Finally, we have selected PA and DMBA for the application to the analysis of CSF extracts. One of them provided high ionization efficiency of nusinersen (Table 1), while the other allowed for the greater nusinersen retention.

3.2.6. Separation attempts

Reliable metabolite identification is challenging if the separation was not optimal (at least partial). The concentration of metabolites is low, and when they co-elute with nusinersen or other metabolites, data interpretation is complex. The deconvoluted signals for nusinersen are

high, while for low-concentration metabolites, very low. Furthermore, some metabolites have a similar molecular mass and result in similar nominal m/z values in mass spectra, e.g. $m/z=1190.2800$ (3'N-6PS) and $m/z=1190.0340$ (3'N-15PS); $m/z=1989.7230$ (3'N-3PS) and $m/z=1989.2065$ (5'N-8); $m/z=1741.0260$ (3'N-9) and $m/z=1741.1587$ (5'N-5PS) (Table S5). If they are coeluted from a chromatographic column, m/z values may overlap, providing an additional source of possible mistakes in the identification (they can be mistakenly identified as one metabolite) [7]. All of these challenges result in data interpretation challenges to find a method to undoubtedly identify metabolites in the coeluting peaks and signals.

Therefore, we have tested PA and DMBA to find optimal conditions allowing good sensitivity (high peak areas) and at least partial separation. An extract obtained from the CSF of P13 (7th dose) was selected for comparison of separation efficiency (Table S1). Figure 2 presents the results of nusinersen metabolites separation attempt obtained for both amines. Only eleven metabolites out of all detected in the extracts were chosen for presentation in the figure, since we wanted to show differences in resolution. It should be underlined that the scales are the same in both Figure 2 A and B, and therefore the EIC chromatograms may be directly compared. The gradient program was changed to obtain similar nusinersen retention. At the same time, it was necessary to use a much lower percentage of MeOH to elute nusinersen out of the chromatographic column, which proves its lower retention in the case of PA (Figure 2A). Generally, the longer the alkyl chain in the structure, as well as the higher order (secondary and tertiary) of amines, the greater is ON retention [10,40]. These effects impact the resolution of metabolites. Separation of 3'N-shortmer metabolites is not possible in the case of PA, unlike DMBA. In this case, we separated at least partially almost all 3'N-shortmers (except for 3'N-1 and 3'N-2) (Figure 2B). The difference in retention time ranged from 0.3 to 0.9 minutes between nusinersen metabolites differing in length by a single nucleotide. On the other hand, the peak shape is broadened when DMBA is used (Figure 2B). Broadening of peaks and lower ionization result in reduced sensitivity in the case of DMBA, compared to PA (Figure 2). However, due to the fact that the highest possible resolution is most important to us in these studies (in order to increase the reliability of identification), we chose DMBA for the analysis of CSF extracts. The separation method was further improved by optimizing the gradient profile. The initial (from 15% v/v) and final (up to 60% v/v) MeOH content were changed without changing the time (15 min). Optimization consisted in changing the gradient slope, which affected the resolution of metabolites. With a decrease in the slope, the resolution increased, but only to a certain extent, because it was observed that a change of less than 18% MeOH in 15 min did not increase the separation, but caused peak asymmetry. As part of refining the method, we have

also improved the column temperature to reduce possible interactions between ONs and hairpin structures, thereby increasing separation. The final selected mobile phase and gradient program provided chromatographic separation.

The developed method enabled the separation of metabolites with similar m/z (mentioned in the former paragraph) of parent ions, which is important for a reliable interpretation. Figure 3 shows an example of the separation of 3'N-9 and 5'N-5PS metabolites. The EIC chromatograms recorded for ions 1741.0263 and 1741.1591 show two peaks, one originating from 3'N-9 and the other from 5'N-5PS (Figure 3). If they were co-eluted, their identification would be difficult. In our studies, we also monitored other ions for selected metabolites to provide additional confirmation. In this case, these were $m/z=1160.4385$ and $m/z=2612.2427$.

3.2.7. MS parameters optimization - Box-Behnken design

Except for IP RP UHPLC conditions, MS conditions were carefully optimized using a design of experiments with a Box-Behnken design. The optimization of nine Q-TOF-MS parameters was performed to increase the sensitivity of nusinersen determination. Therefore peak area at the EIC chromatogram for $m/z = 2374.420$ was selected as the dependent variable. Although we did not perform quantitative analysis, high sensitivity was essential for detecting the highest possible number of its metabolites. As peak area results from ionization efficiency, and it is related to MS parameters, three sets of independent variables were studied: 1. DGT, SGT, OV, 2. NGP, DGF, SGF, 3. SV, CV, FV. A total of 13 chromatographic runs (in replicates) were found to be sufficient to perform complete optimization. Their results are collected in Table S2. The results were used for response surface modelling and Figure S1 presents a two-dimensional contour plot for optimization of three sets of values using CCD. As can be seen in Figure S1A, SGT and DGT should have high values (preferably above 350), with the former being higher than the latter. At the same time, OV should be set to the highest possible value, as this results in large peak areas for nusinersen on the EIC (Figure S1A). Comparing the effect of gas flow at the ion source (Figure S1B), both should be high, with SGF once again needing to be higher than DGF to achieve higher sensitivity. The dependence of NGP on gas flow rates is analogous for both of them (Figure S1B). The highest EIC peak surface areas are observed either for low SGF and DGF values (7.5 or 1.0 L min^{-1} , respectively) and 40 psi, or for high SGF and DGF values and NGP in the range of 45-50 psi (Figure S1B). Neither high nor low NGP values allow for effective ionization of nusinersen, leading to large peak areas (increased sensitivity). Based on Figure S1C, we can conclude that FV should be higher than 250V, preferably around 300V (due to CV). At the same time, SV should not exceed

100 V (Figure S1C). As for CV, theoretically (based on the graphs), either a low (2800V) or a high value (5000V) should be applied (Figure S1C). Unfortunately, neither of these values is optimal in terms of sensitivity, as CV correlates with SV and FV in a different (opposite) way (Figure S1C). The choice of the final CV values was a compromise. Ultimately, the following values were selected: SGT 400°C, DGT 360°C, OV 800V, SGF 12 L min⁻¹, DGF 10 L min⁻¹, NGP 48psi, FV 300V, SV 80V, CV 4500V.

3.3. Sample preparation

So far, a noncompetitive hybridization nuclease-based enzyme-linked immunosorbent assay (ELISA) method and an electrochemiluminescence (ECL) method have been applied to quantify nusinersen in CSF samples (without sample preparation). These techniques showed high sensitivity (0.05-1.5 ng/mL), but they cannot be used for the identification of any of the metabolites [1]. One of the latest studies presented a successful application of simple protein precipitation using acetonitrile with 0.3% TEA for the extraction of nusinersen [5]. However, our findings do not support this result, especially in the case of metabolites, whose concentration is very low in CSF. Furthermore, to our knowledge, nusinersen undergoes co-precipitation with proteins. Other studies confirmed the usefulness of SPE for nusinersen extraction from CSF with recoveries ranging from 93 to 96% and matrix effect of 90%, suggesting the need for additional purification [3,8]. Despite its applicability, SPE has never been used for the isolation of metabolites. We wanted to extend and prove its utility for nusinersen metabolites with very low concentration.

LLE using a phenol/chloroform/isoamyl alcohol mixture was used to separate proteins from ONs. This extraction simultaneously removes chloroform-soluble lipid residues. However, extracts obtained after LLE contain residues of phenol, peptides, and other compounds present in CSF. Furthermore, our previous studies [7,15,30] have shown that LLE extraction alone is insufficient to detect nusinersen or its metabolites in the LLE extract, because concentration and purification are needed. SPE was used for this purpose. The entire procedure was carried out in ion pair mode, as previous studies have proven its usefulness in isolating ONs from biological samples [21,42,43]. A mixture of HA and HFIP was used because this amine adsorbs more effectively on the surface of adsorbents and forms ion pairs with ON, reducing their polarity and increasing their affinity for the adsorbent [20]. These two effects are important during the extraction of nusinersen and its metabolites from CSF. LLE extracts were diluted with HA/HFIP solution before SPE (in a 1:1 v/v ratio) to form ion pairs between HA

and nusinersen metabolites before sample load. Such an attempt increases the extraction efficiency, due to complete adsorption during sample loading to the SPE cartridge.

In the preliminary studies, the CSF sample was fortified with nusinersen to a concentration of 0.05 μ M. LLE and SPE extracts (before evaporation) were analyzed using the developed IP RP UHPLC Q-TOF-MS method. At the same time, the ME was determined for each stage (LLE and SPE, respectively). The LLE recovery was equal to 94.1 \pm 4.2%, with ME equal to 89%. Recovery is high, but reproducibility is low. Additionally, the ME indicates the need for additional purification of the extract (the presence of other compounds from the matrix that affect the determination of nusinersen). The following SPE procedure provided a recovery of 89.2 \pm 1.8% with no ME (equal to 100%). Additionally, the eluates were collected from the cartridge after sample load and after washing. No nusinersen was detected in any of the eluates, indicating its complete adsorption. The results prove the method's usefulness in nusinersen extraction and the importance of the second extraction step to purify the extract and increase reproducibility. Moreover, evaporation of SPE extract to dryness and reconstitution of the residue in 50 μ L of mobile phase did not reduce recovery and reproducibility (nusinersen is stable at 40 $^{\circ}$ C), while enabling 50-fold sample concentration (from 2.5 mL of CSF sample to 50 μ L of extract). In our opinion, the two-step sample preparation method is effective (high recovery from biological samples) and reproducible (low standard deviation). This makes it useful for the analysis of nusinersen and its potential metabolites in CSF samples.

In the next stage of the study, the developed LLE SPE procedure was applied to the analysis of samples collected from patients with SMA (Table S1). Extracts obtained after both LLE extraction and SPE purification were analyzed. Neither nusinersen nor its metabolites were detected. The 50-fold concentration of extracts enabled the detection of these compounds. These results suggest that the concentration of both the nusinersen and its metabolites in CSF samples is very low. This effect is probably related to the fact that samples were taken 4 months after the last dose of Spinraza. This drug is administered first by 4 loading doses on days 0, 14, 28, and 63, and next a maintenance dose is administered once every 4 months (maintaining a constant concentration of nusinersen in the central nervous system). Consequently, the amount of nusinersen before administration of the next dose may be low, as indicated by our study.

3.6. Nusinersen metabolites in CSF samples of patients with SMA

Table S6 lists all metabolites detected using the developed analytical procedure (from sample preparation through separation to identification). Figure 4 shows example EIC chromatograms for a sample extracted from patient P6 before the 18th dose of the drug. The

upper figure shows the superimposed chromatograms of metabolites and nusinersen, while the lower figure shows the chromatograms for the metabolites alone. These results show that, for a sample with many metabolites, partial separation is achieved, but their identification remains possible. For this purpose, ions with m/z higher than 2000 were most often selected for monitoring, as there were no ions with similar m/z in this range (such as $m/z=1190$ for 3'N-6PS and 3'N-15PS; or $m/z=1989$ 3'N-3PS and 5'N-8), which allows for greater specificity (Table S5). This was not possible in every case because, as the metabolite's mass decreased, the observed m/z values also decreased (Table S5). Table 2 shows the predicted and observed deconvoluted masses of metabolites detected in the CSF extracts.

As shown in Tables 2 and S5, nusinersen is metabolized in the CSF over the four months between successive doses of Spinraza, and the number of metabolites differs among patients. A progressive exonucleolytic degradation of nusinersen is not beneficial because it reduces the therapeutic effect, as only the full-length nusinersen sequence provides a high therapeutic effect. We would like to strongly emphasize that, to the best of our knowledge, this is one of the first publications in which LLE SPE IP RP UHPLC Q-TOF-MS has been successfully used for the extraction, separation, and identification of nusinersen metabolites in CSF samples from children with SMA treated with Spinraza. It is also one of the few publications in which these techniques have been applied not only to antisense ON standards (or fortified biological samples) but also to patient samples from those treated with therapeutic ONs. The novelty lies not in the detection of nusinersen itself, but in demonstrating that, with appropriate sample preparation, we can extend the applicability of the developed method to metabolites. This is important for monitoring the metabolism of nusinersen and therapeutic effects, and, in the future, to the patient's condition.

Regrettably, we did not have CSF samples from patients collected at the start of therapy (Table S1). This makes it impossible to conclude whether nusinersen metabolism changes between the first initial doses and subsequent maintenance doses. We cannot conclude whether there is a difference between the initial stage of therapy and subsequent months. In general, N-shortmers were observed, with 3'N-shortmers being more abundant than metabolites shorter by consecutive nucleotides from the 5' end (Figure 4, Table S6). Unfortunately, for most patients and samples, we cannot make a direct comparison of the data because either we do not have samples from the same dose, or the patients have a different type of SMA, or they started treatment at a different age, etc. At this stage, we cannot draw general conclusions about the correlation between therapeutic effect and metabolism. What is clear, however, is that in the case of children who began therapy at ages 9 and 10 (P3, P4, P8), the number of metabolites is

lower (Table S6). Still, we need more patients from whom we can collect, analyze, and monitor samples from the start of therapy. The number of patients (17) involved in this study is not enough to draw general conclusions. However, one tendency was observed and confirmed, namely identification of nusinersen up to a certain stage of treatment. Nusinersen was not detected in all CSF samples (Table S6), especially in samples after the 14th dose of the drug, except for P1 and P3, in which nusinersen was no longer detected after the 10th dose (Table S6). On the other hand, for P2, P4, P5, P6, P7, and P13, nusinersen was detected even after 15th dose, indicating that the presence of nusinersen in CSF and its metabolism depend on the patient (Table S6). The LOQ for the nusinersen and developed IP RP UHPLC Q-TOF-MS method is 0.01 μM ; consequently, in samples where we did not detect nusinersen, its concentration was below 0.01 μM (0.2 nM if we take into account the concentration). It appears that nusinersen, depending on the patient and the dose of the drug, begins to be used up entirely or completely metabolized, and its concentration in CSF at a certain point during therapy is extremely low (our method does not allow for its detection). Patients then report feeling worse (lack of strength, weakness) before the next dose of the drug is administered. Here, we observe a correlation between the patient's weakness and the undetectability of nusinersen in the CSF.

Furthermore, the number and type of metabolites vary depending on both the patient and the dose of the drug. Virtually every sample contains 3'N-1, 5'N-1 (or 5'N-1PS), and usually also 3'N-2. However, the remaining metabolites vary between patients (Table S6). A fixed-dose scheme of 12 mg across all age groups, SMA types, and dose number was used when the samples used during the present study were collected [1]. Since January 2026, the EMA (and previously the FDA) has approved the use of higher doses of nusinersen: 28 mg (maintenance dose) and 50 mg (loading phase, two doses). Physicians should decide on a case-by-case basis whether to use them. Our results suggest that probably the increase of nusinersen amount should be considered at various stages of treatment for different patients, as indicated by our results (Table S6), e.g., for some patients nusinersen is detectable even before 20th dose. At the same time, for other children it is not detectable as quickly as before 10th dose. Furthermore, it may be advisable to introduce routine CSF nusinersen level measurements in children treated with Spinraza in hospitals (e.g., at each dose). Such monitoring would make it possible to determine when the drug dose should be increased in a more complex and reliable manner.

However, there is still insufficient data to identify statistically significant correlations between the detection of nusinersen, identified metabolites, and the type of SMA or the patient's condition (breathing, nutrition). Our research is ongoing to determine whether such correlations exist in the next stage. It will be continued for the next two years. We hope that at the end of

this study, based on the data obtained, we will be able to indicate whether there are any correlations between metabolism and nusinersen concentration, the dose of the drug, the type of SMA, and the patient's condition.

4. Conclusions

A comprehensive analytical procedure was successfully developed for the extraction, separation, and identification of nusinersen metabolites in CSF samples from children with SMA treated with Spinraza. To our knowledge, this is the first study demonstrating the applicability of LLE/SPE and IP RP UHPLC Q-TOF-MS to nusinersen metabolism study in real CSF samples. Nusinersen showed relatively high physicochemical stability under various storage and freeze-thaw conditions, ensuring reliable sample handling and analysis.

To sum up, there are three key issues in preparing CSF samples for analysis of nusinersen and its metabolites several months after intrathecal administration: reproducibility (necessary for the analysis of biological sample to identify unknown metabolites), purification (reduction of the matrix effect suppressing ionization in MS), and significant (more than 40-fold) sample concentration (necessary only when CSF was collected several months after drug administration). Each of these key issues is addressed in the method we have developed. Moreover, the LLE/SPE allows the extraction of both nusinersen and all metabolites, not only nusinersen. LLE enables the removal of proteins and lipids, whereas subsequent SPE enhances purification, reproducibility, and analyte recovery.

Furthermore, careful optimization of chromatographic and MS parameters is essential for the detection, separation, and identification of nusinersen and its metabolites. Reliable metabolite identification depends on sufficient chromatographic resolution, particularly when metabolites differ by a single nucleotide and may exhibit similar nominal m/z values. The ion-pair reagent selection remains the key parameter during optimization of separation and increasing the sensitivity in order to enable the detection of low-abundance metabolites. The shallow gradient is necessary to obtain metabolite separation. Although we have selected DMBA, it should be noted that PA provides greater sensitivity. If complete separation of metabolites is not necessary, then this ion pair reagent may be routinely used. Utilization of accurate Q-TOF-MS allows identification of nusinersen metabolites, and additional identification specificity is provided by characteristic structural elements of nusinersen modifications. They are beneficial because sequence-specific fragment ions (modified nucleobase, phosphorothioate group) are observed during MS/MS fragmentation, confirming the presence of nusinersen metabolites in the complex CSF matrix.

The multiple N-shortmer metabolites, predominantly 3'-truncated ones, were identified in patient CSF samples, confirming that nusinersen undergoes metabolism in the central nervous system between maintenance doses. Considerable interpatient variability was observed in both nusinersen detection and metabolite profiles. Preliminary observations indicate a possible relationship between low or undetectable nusinersen levels and clinical deterioration before the next administration, highlighting the potential value of therapeutic drug monitoring and individualized dosing strategies. The developed methodology expands the bioanalytical toolbox for antisense oligonucleotides and provides a foundation for future studies investigating correlations between metabolism, drug exposure, dosing regimen, and clinical response in SMA therapy.

Acknowledgements

The authors are grateful to National Science Centre (Cracow, Poland) for financial support under Opus project (2023/51/B/NZ7/00537).

Author contribution statement:

Sylwia Studzińska: conceptualization, methodology, investigation, resources, data curation, writing – original draft, project administration, funding acquisition

Maria Mazurkiewicz-Beldzińska: sample collection, writing – review and editing

Anna Lemska: sample collection, writing– review and editing

Jakub Szymarek: sample collection, writing – review and editing

Declarations

Samples were taken in accordance with the relevant guidelines of the Medical University of Gdańsk and approved by the Independent Bioethics Committee for Scientific Research at the Medical University of Gdańsk (permission no. NKBBN/778/2022).

References

- [1] K.T. Luu, D.A. Norris, R. Gunawan, S. Henry, R. Geary, Y. Wang, Population Pharmacokinetics of Nusinersen in the Cerebral Spinal Fluid and Plasma of Pediatric Patients With Spinal Muscular Atrophy Following Intrathecal Administrations, *The Journal of Clinical Pharmacology* 57 (2017) 1031–1041. <https://doi.org/10.1002/jcph.884>.

- [2] N.K. Mishra, A. Mishra, Spinal Muscular Atrophy (SMA): Treatment strategies, challenges and future prospects, *Pharmacological Research - Reports* 3 (2025) 100031. <https://doi.org/10.1016/j.prerep.2025.100031>.
- [3] Y. Li, S. Zhang, X. Wang, X. Li, L. Guo, LC-MS/MS quantification of nusinersen in rat cerebrospinal fluid and preclinical pharmacokinetics study application, *Bioanalysis* 17 (2025) 839–846. <https://doi.org/10.1080/17576180.2025.2535949>.
- [4] X. Zhang, C. Sha, W. Zhang, F. Zhao, M. Zhu, G. Leng, W. Liu, Development, Validation and Application of an Ion-Pair Reversed-Phase Liquid Chromatography-Tandem Mass Spectrometry Method for the Quantification of Nusinersen, *Bioanalysis* 16 (2024) 305–317. <https://doi.org/10.4155/bio-2023-0218>.
- [5] T. Xu, W. Zuo, Z. Sun, S. Zhang, Z. Qiu, B. Zhang, Y. Dai, Development and Validation of an LC–MS/MS Assay for Quantitative Analysis of Nusinersen in Human CSF and Plasma, *Biomedical Chromatography* 39 (2025). <https://doi.org/10.1002/bmc.70138>.
- [6] E.E. Neil, E.K. Bisaccia, Nusinersen: A Novel Antisense Oligonucleotide for the Treatment of Spinal Muscular Atrophy, *The Journal of Pediatric Pharmacology and Therapeutics* 24 (2019) 194–203. <https://doi.org/10.5863/1551-6776-24.3.194>.
- [7] S. Studzińska, M. Mazurkiewicz-Beldzińska, B. Buszewski, Development of the Method for Nusinersen and Its Metabolites Identification in the Serum Samples of Children Treated with Spinraza for Spinal Muscular Atrophy, *Int. J. Mol. Sci.* 23 (2022). <https://doi.org/10.3390/ijms231710166>.
- [8] X. Zhang, C. Sha, W. Zhang, F. Zhao, M. Zhu, G. Leng, W. Liu, Development and validation of an HILIC/MS/MS method for determination of nusinersen in rabbit plasma, *Heliyon* 10 (2024) e31213. <https://doi.org/10.1016/J.HELIYON.2024.E31213>.
- [9] S. Studzińska, Review on investigations of antisense oligonucleotides with the use of mass spectrometry, *Talanta* 176 (2018). <https://doi.org/10.1016/j.talanta.2017.08.025>.
- [10] A. Kaczmarkiewicz, Ł. Nuckowski, S. Studzińska, B. Buszewski, Analysis of Antisense Oligonucleotides and Their Metabolites with the Use of Ion Pair Reversed-Phase Liquid Chromatography Coupled with Mass Spectrometry, *Crit. Rev. Anal. Chem.* 49 (2019). <https://doi.org/10.1080/10408347.2018.1517034>.
- [11] G.J. Guimaraes, M.G. Bartlett, Managing nonspecific adsorption to liquid chromatography hardware: A review, *Anal. Chim. Acta* 1250 (2023). <https://doi.org/10.1016/j.aca.2023.340994>.

- [12] T. Kessler, P. Latzer, D. Schmid, U. Warnken, A. Saffari, A. Ziegler, J. Kollmer, M. Möhlenbruch, C. Ulfert, C. Herweh, B. Wildemann, W. Wick, M. Weiler, Cerebrospinal fluid proteomic profiling in nusinersen-treated patients with spinal muscular atrophy, *J. Neurochem.* 153 (2020). <https://doi.org/10.1111/jnc.14953>.
- [13] Y. Zhan, J. Guo, P. Hu, R. Huang, J. Ning, X. Bao, H. Chen, Z. Yan, L. Ding, C. Shu, A sensitive analytical strategy of oligonucleotide functionalized fluorescent probes for detection of nusinersen sodium in human serum, *Talanta* 275 (2024) 126153. <https://doi.org/10.1016/j.talanta.2024.126153>.
- [14] S. Studzińska, O. Błachowicz, S. Bocian, O. Kalisz, A. Jaworska, J. Szymarek, M. Mazurkiewicz-Beldzińska, Study of nusinersen metabolites in the cerebrospinal fluid of children with spinal muscular atrophy using ultra-high-performance liquid chromatography coupled with quadrupole-time-of-flight mass spectrometry, *Analyst* 149 (2024). <https://doi.org/10.1039/d4an00436a>.
- [15] S. Studzińska, J. Szymarek, M. Mazurkiewicz-Beldzińska, Improvement of serum sample preparation and chromatographic analysis of nusinersen used for the treatment of spinal muscular atrophy, *Talanta* 267 (2024). <https://doi.org/10.1016/j.talanta.2023.125173>.
- [16] M. Garofalo, S. Bonanno, S. Marcuzzo, C. Pandini, E. Scarian, F. Dragoni, R. Di Gerlando, M. Bordoni, S. Parravicini, C. Gellera, R. Masson, C. Dosi, R. Zanin, O. Pansarasa, C. Cereda, A. Berardinelli, S. Gagliardi, Preliminary insights into RNA in CSF of pediatric SMA patients after 6 months of nusinersen, *Biol. Direct* 18 (2023). <https://doi.org/10.1186/s13062-023-00413-6>.
- [17] R. Orbach, L. Sagi, E. Sadot, I. Tokatly Latzer, A. Shtamler, T. Zisberg, A. Fattal-Valevski, Cerebrospinal fluid characteristics of patients treated with intrathecal nusinersen for spinal muscular atrophy, *Muscle Nerve* 66 (2022). <https://doi.org/10.1002/mus.27731>.
- [18] G. Cebulla, L. Hai, U. Warnken, C. Güngör, D.C. Hoffmann, M. Korporeal-Kuhnke, B. Wildemann, W. Wick, T. Kessler, M. Weiler, Long-term CSF responses in adult patients with spinal muscular atrophy type 2 or 3 on treatment with nusinersen, *J. Neurol.* 272 (2025). <https://doi.org/10.1007/s00415-025-12984-7>.
- [19] D. Li, N. Sun, H. Wu, X. Wang, Y. Shi, L. Yang, S. Huang, K. Zhang, C. Yang, Cerebrospinal fluid metabolomics reveals predictive biomarkers of nusinersen therapy efficacy in type II and type III spinal muscular atrophy patients, *Neurological Sciences* 46 (2025). <https://doi.org/10.1007/s10072-025-08267-8>.
- [20] Ł. Nuckowski, A. Kaczmarkiewicz, S. Studzińska, Development of SPE Method for the Extraction of Phosphorothioate Oligonucleotides from Serum Samples, *Bioanalysis* 10 (2018) 1667–1677. <https://doi.org/10.4155/bio-2018-0166>.

- [21] W. Zhang, N. Leighl, D. Zawisza, M.J. Moore, E.X. Chen, Determination of GTI-2040, a novel antisense oligonucleotide, in human plasma by using HPLC combined with solid phase and liquid–liquid extractions, *Journal of Chromatography B* 829 (2005) 45–49. <https://doi.org/10.1016/j.jchromb.2005.09.036>.
- [22] <https://numiqo.com/statistics-calculator/design-of-experiments>, (n.d.).
- [23] G.J. Guimaraes, J.M. Sutton, M. Gilar, M. Donegan, M.G. Bartlett, Impact of Nonspecific Adsorption to Metal Surfaces in Ion Pair-RP LC-MS Impurity Analysis of Oligonucleotides, *J. Pharm. Biomed. Anal.* 208 (2022). <https://doi.org/10.1016/j.jpba.2021.114439>.
- [24] H. Lardeux, A. Goyon, K. Zhang, J.M. Nguyen, M.A. Lauber, D. Guillaume, V. D’Atri, The impact of low adsorption surfaces for the analysis of DNA and RNA oligonucleotides, *J. Chromatogr. A* 1677 (2022). <https://doi.org/10.1016/j.chroma.2022.463324>.
- [25] J.M. Nguyen, M. Gilar, B. Koshel, M. Donegan, J. MacLean, Z. Li, M.A. Lauber, Assessing the Impact of Nonspecific Binding on Oligonucleotide Bioanalysis, *Bioanalysis* 13 (2021) 1233–1244. <https://doi.org/10.4155/bio-2021-0115>.
- [26] H. Lardeux, K. Stavenhagen, C. Paris, R. Dueholm, C. Kurek, L. De Maria, F. Gnerlich, T. Leek, W. Czechtizky, D. Guillaume, M. Jora, Unravelling the Link between Oligonucleotide Structure and Diastereomer Separation in Hydrophilic Interaction Chromatography, (2024). <https://doi.org/10.1021/acs.analchem.4c01384>.
- [27] J.M. Sutton, N.M. El Zahar, M.G. Bartlett, Oligonucleotide Anion Adduct Formation Using Negative Ion Electrospray Ion-Mobility Mass Spectrometry, *J. Am. Soc. Mass Spectrom.* 32 (2021) 497–508. <https://doi.org/10.1021/jasms.0c00380>.
- [28] J. Kim, B. Basiri, C. Hassan, C. Punt, E. van der Hage, C. den Besten, M.G. Bartlett, Metabolite Profiling of the Antisense Oligonucleotide Eluforsen Using Liquid Chromatography-Mass Spectrometry, *Mol. Ther. Nucleic Acids* 17 (2019). <https://doi.org/10.1016/j.omtn.2019.07.006>.
- [29] B. Chen, S.F. Mason, M.G. Bartlett, The Effect of Organic Modifiers on Electrospray Ionization Charge-State Distribution and Desorption Efficiency for Oligonucleotides, *J. Am. Soc. Mass Spectrom.* 24 (2013) 257–264. <https://doi.org/10.1007/s13361-012-0509-5>.
- [30] A. Kilanowska, Ł. Nuckowski, S. Studzińska, Studying in vitro metabolism of the first and second generation of antisense oligonucleotides with the use of ultra-high-performance liquid chromatography coupled with quadrupole time-of-

- flight mass spectrometry, *Anal. Bioanal. Chem.* 412 (2020).
<https://doi.org/10.1007/s00216-020-02878-0>.
- [31] A. Kaczmarkiewicz, Ł. Nuckowski, S. Studzińska, Analysis of the first and second generation of antisense oligonucleotides in serum samples with the use of ultra high performance liquid chromatography coupled with tandem mass spectrometry, *Talanta* 196 (2019) 54–63.
<https://doi.org/10.1016/j.talanta.2018.12.023>.
- [32] K.J. Fountain, M. Gilar, J.C. Gebler, Analysis of native and chemically modified oligonucleotides by tandem ion-pair reversed-phase high-performance liquid chromatography/electrospray ionization mass spectrometry, *Rapid Communications in Mass Spectrometry* 17 (2003) 646–653.
<https://doi.org/10.1002/rcm.959>.
- [33] M. Gilar, K.J. Fountain, Y. Budman, J.L. Holyoke, H. Davoudi, J.C. Gebler, Characterization of Therapeutic Oligonucleotides Using Liquid Chromatography with On-line Mass Spectrometry Detection, *Oligonucleotides* 13 (2003) 229–243. <https://doi.org/10.1089/154545703322460612>.
- [34] J. Kim, N.M. El Zahar, M.G. Bartlett, *In vitro* metabolism of 2'-ribose unmodified and modified phosphorothioate oligonucleotide therapeutics using liquid chromatography mass spectrometry, *Biomedical Chromatography* 34 (2020). <https://doi.org/10.1002/bmc.4839>.
- [35] A.C. McGinnis, E.C. Grubb, M.G. Bartlett, Systematic optimization of ion-pairing agents and hexafluoroisopropanol for enhanced electrospray ionization mass spectrometry of oligonucleotides, *Rapid Communications in Mass Spectrometry* 27 (2013) 2655–2664. <https://doi.org/10.1002/rcm.6733>.
- [36] L. Gong, J.S.O. McCullagh, Comparing ion-pairing reagents and sample dissolution solvents for ion-pairing reversed-phase liquid chromatography/electrospray ionization mass spectrometry analysis of oligonucleotides, *Rapid Communications in Mass Spectrometry* 28 (2014) 339–350. <https://doi.org/10.1002/rcm.6773>.
- [37] B. Basiri, H. van Hattum, W.D. van Dongen, M.M. Murph, M.G. Bartlett, The Role of Fluorinated Alcohols as Mobile Phase Modifiers for LC-MS Analysis of Oligonucleotides, *J. Am. Soc. Mass Spectrom.* 28 (2017) 190–199.
<https://doi.org/10.1007/s13361-016-1500-3>.
- [38] S.M. McCarthy, M. Gilar, J. Gebler, Reversed-phase ion-pair liquid chromatography analysis and purification of small interfering RNA, *Anal. Biochem.* 390 (2009) 181–188. <https://doi.org/10.1016/j.ab.2009.03.042>.
- [39] B. Basiri, M.G. Bartlett, LC-MS of oligonucleotides: Applications in biomedical research, *Bioanalysis* 6 (2014). <https://doi.org/10.4155/bio.14.94>.

- [40] N. Li, N.M. El Zahar, J.G. Saad, E.R.E. van der Hage, M.G. Bartlett, Alkylamine ion-pairing reagents and the chromatographic separation of oligonucleotides, *J. Chromatogr. A* 1580 (2018) 110–119. <https://doi.org/10.1016/j.chroma.2018.10.040>.
- [41] B. Basiri, M.M. Murph, M.G. Bartlett, Assessing the Interplay between the Physicochemical Parameters of Ion-Pairing Reagents and the Analyte Sequence on the Electrospray Desorption Process for Oligonucleotides, *J. Am. Soc. Mass Spectrom.* 28 (2017) 1647–1656. <https://doi.org/10.1007/s13361-017-1671-6>.
- [42] Y. Cen, X. Li, D. Liu, F. Pan, Y. Cai, B. Li, W. Peng, C. Wu, W. Jiang, H. Zhou, Development and validation of LC–MS/MS method for the detection and quantification of CpG oligonucleotides 107 (CpG ODN107) and its metabolites in mice plasma, *J. Pharm. Biomed. Anal.* 70 (2012) 447–455. <https://doi.org/10.1016/j.jpba.2012.06.022>.
- [43] R. Erb, K. Leithner, A. Bernkop-Schnürch, H. Oberacher, Phosphorothioate Oligonucleotide Quantification by μ -Liquid Chromatography-Mass Spectrometry, *AAPS J.* 14 (2012) 728–737. <https://doi.org/10.1208/s12248-012-9381-2>.

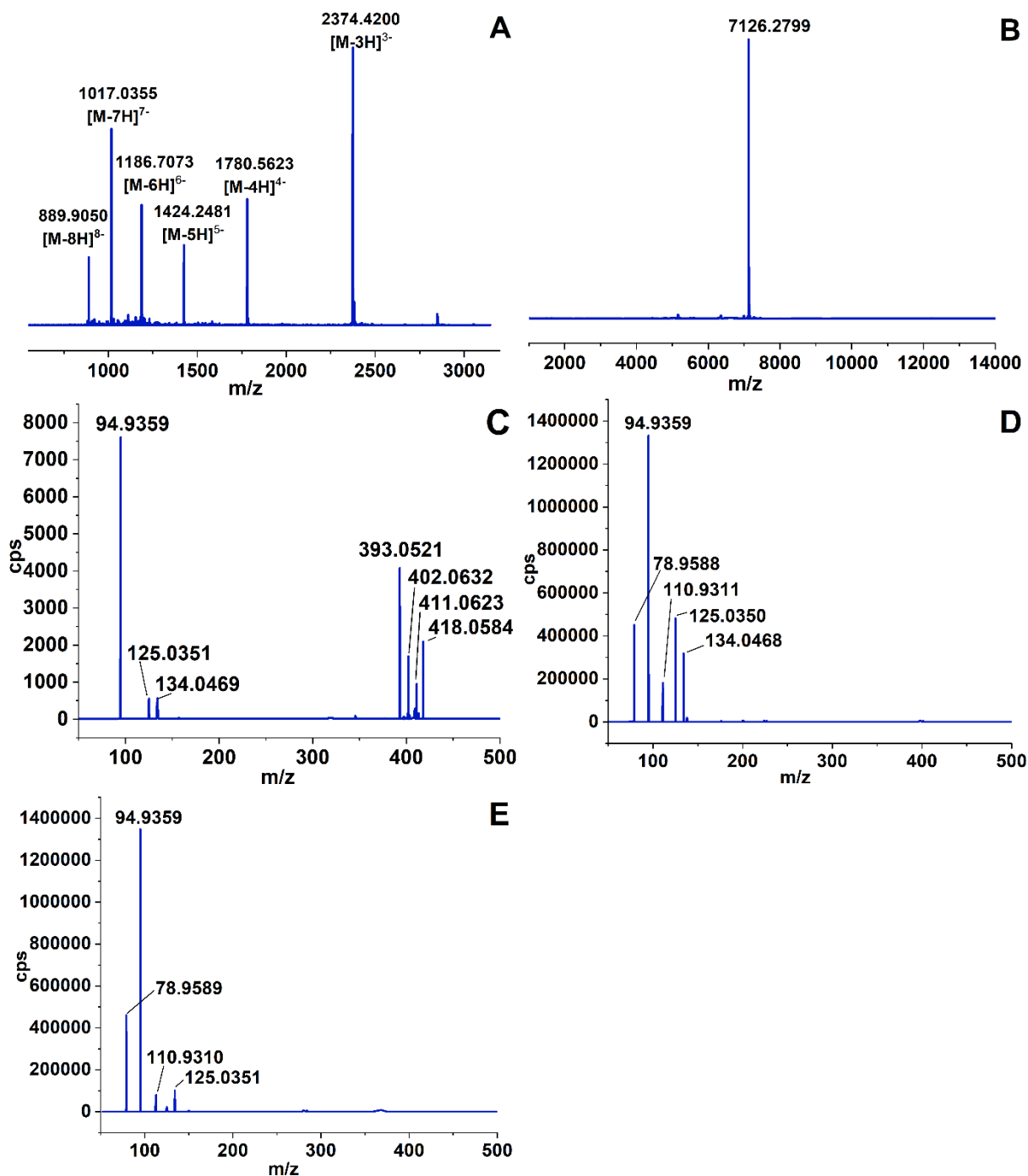


Figure 1. Mass spectra of nusinersen standard: A) full scan mass spectra, B) deconvoluted mass spectra, C) fragmentation mass spectra recorded for collision energy equal to 10 eV, D) fragmentation mass spectra recorded for collision energy equal to 100 eV, E) fragmentation mass spectra recorded for collision energy equal to 190 eV.

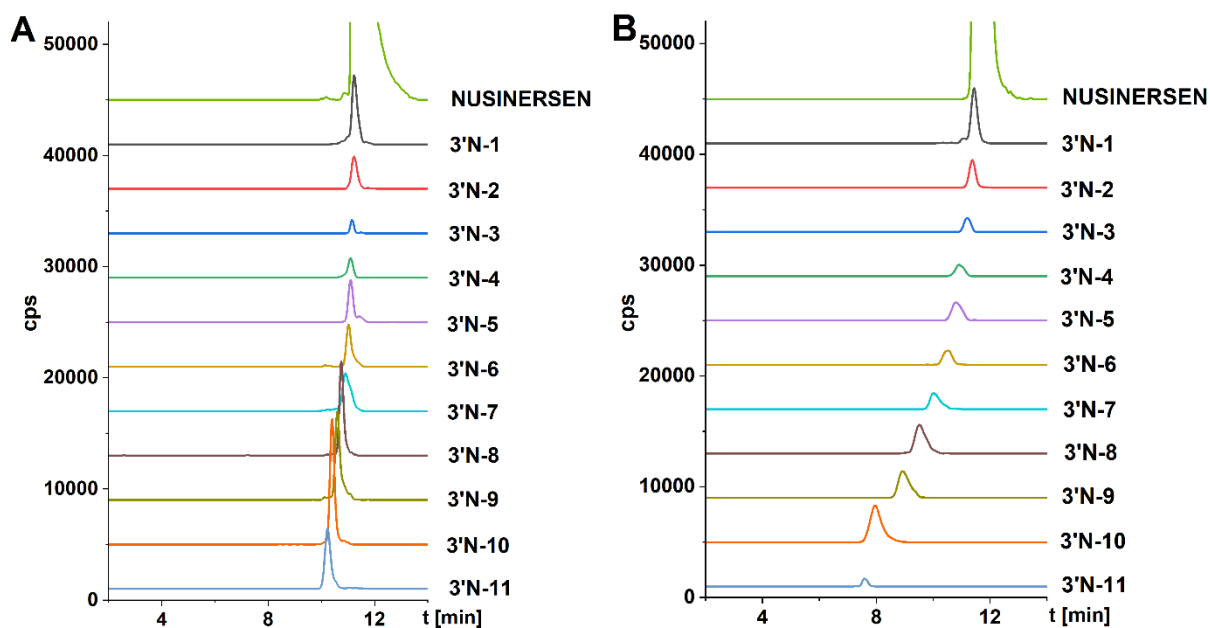


Figure 2. Representative extracted ion chromatograms of a full-length nusinersen and its 3'-N-shortmer metabolites in CSF extract of P13 (7th dose) for the following chromatographic conditions: A) 5mM PA/150mM HFIP/MeOH, gradient elution program: 10-30% v/v MeOH in 15min.; B) 5mM DMBA/150mM HFIP/MeOH, gradient elution program: 24-45% v/v MeOH in 15min. Flow rate 0.3 ml min⁻¹. Column temperature 60 °C, autosampler temperature 10 °C.

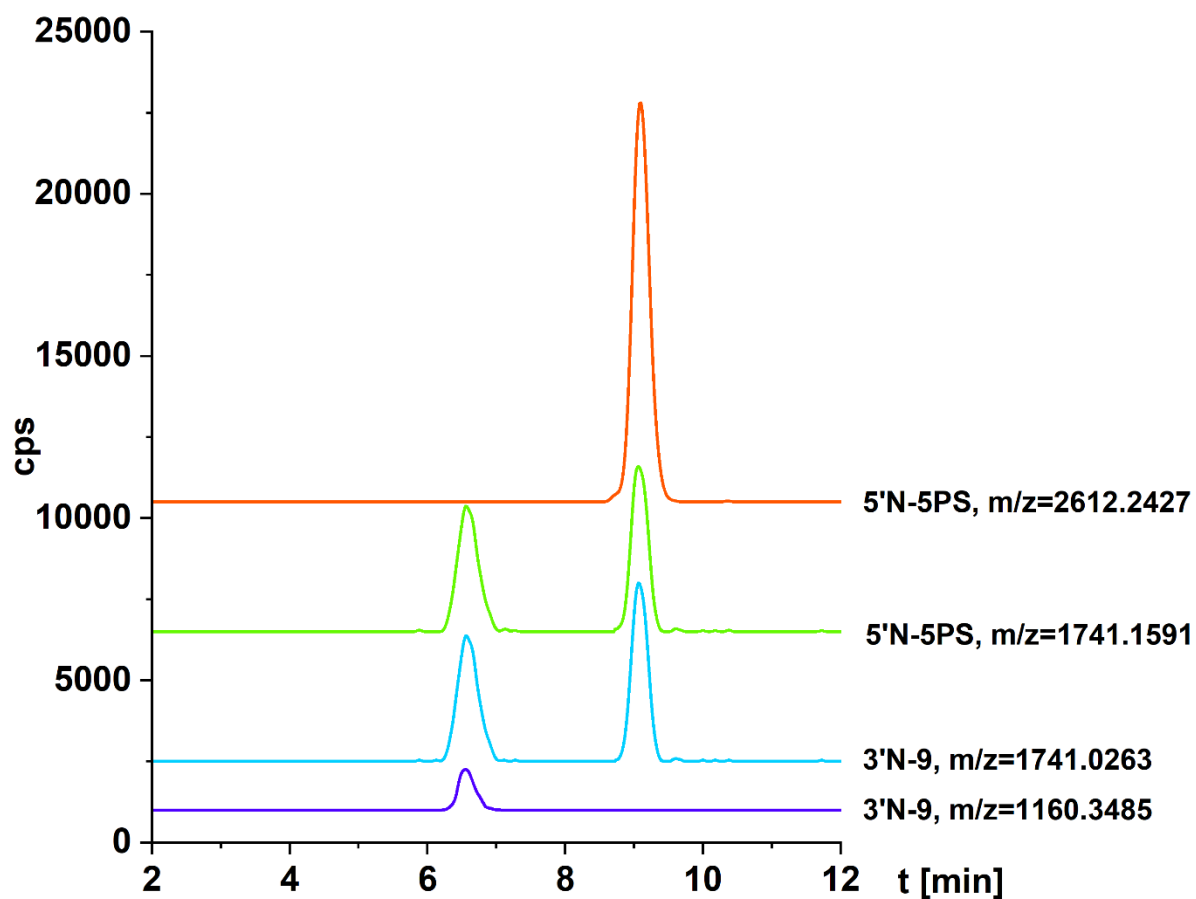


Figure 3. Extracted ion chromatograms for two selected metabolites 5'N-5PS and 3'N-9 and two m/z values for each one of them. Experimental conditions: mobile phase composition: 5mM DMBA/150mM HFIP and MeOH, gradient elution program: 26-44% v/v MeOH v/v MeOH in 15min.

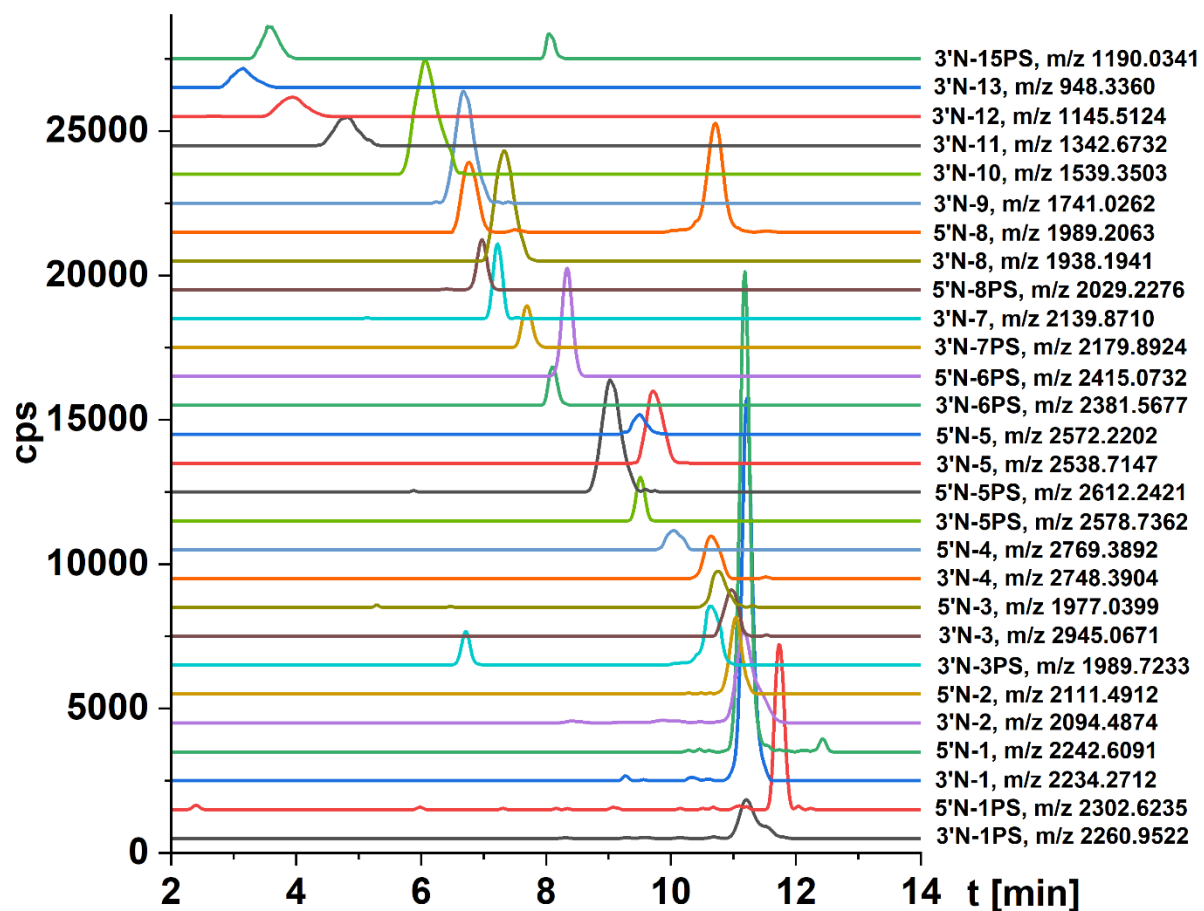
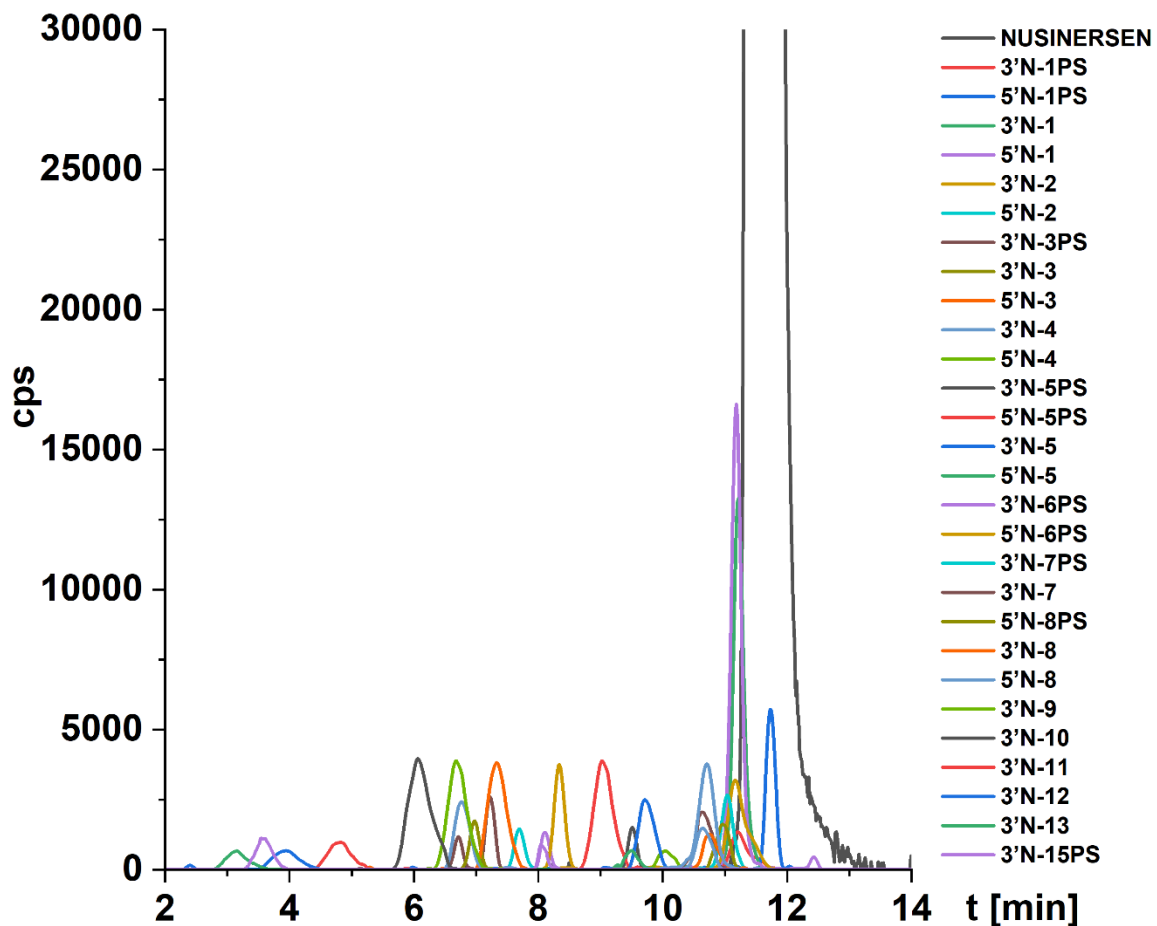


Figure 4. Representative extracted ion chromatograms of a full-length nusinersen and its metabolites detected in CSF extract of P6 (18th dose). Experimental conditions: mobile phase composition: 5mM DMBA/150mM HFIP and MeOH, gradient elution program: 26-44% v/v MeOH v/v MeOH in 15min; flow rate 0.3 ml min⁻¹; column temperature 60 °C; autosampler temperature 10 °C; injection volume 2.5µL; mass spectrometry conditions: nebulizer gas pressure 48 psi, skimmer voltage 80V, capillary voltage 4500V, fragmentor voltage 300V; drying gas flow 10 L min⁻¹; shielding gas flow 10 L min⁻¹; octopole voltage 800V; drying gas temperature 360°C; shielding gas temperature 400 °C.

Table 1. Comparison of peak areas at extracted ion chromatograms (A_{EIC}) for 5 μ M nusinersen standard ($m/z=1017.035$) analyzed using various amines. Mobile phase composition: 50/50% v/v 5 mM amine and 150 mM HFIP/MeOH, injection volume 1 μ L.

Amine	A_{EIC}	Boiling point [$^{\circ}$ C]	Henry's law constant [μ mol/(Pa \cdot kg)]
PA	8603726 \pm 2481	50	660
DEA	8555970 \pm 3755	58	150
HA	3209793 \pm 2977	132	110
DMBA	7264360 \pm 4309	101	115
DIPEA	8005984 \pm 2287	127	65

Table 2. The m/z values for observed ions, predicted and deconvoluted mass, and identified metabolites.

Selected, observed parent ions [m/z]	Charge state	Metabolite			
		Deconvoluted mass [Da]	Calculated mass [Da]	Sequence	Identified metabolite
2260.9522	-3	6785.8801	6785.8810	mU*mC*A*mC*mU*mU*mU*mC*A*mU*A*A*mU*G*mC*mU*G*	3'N-1PS
1356.1679	-5				
2234.2711	-3	6705.8374	6705.8380	mU*mC*A*mC*mU*mU*mU*mC*A*mU*A*A*mU*G*mC*mU*G	3'N-1
1340.1595	-5				
2121.1687	-3	6366.5308	6366.5300	mU*mC*A*mC*mU*mU*mU*mC*A*mU*A*A*mU*G*mC*mU*	3'N-2PS
1272.2983	-5				
2094.4874	-3	6286.4869	6286.4870	mU*mC*A*mC*mU*mU*mU*mC*A*mU*A*A*mU*G*mC*mU	3'N-2
1256.2895	-5				
1989.7234	-3	5972.1921	5972.1930	mU*mC*A*mC*mU*mU*mU*mC*A*mU*A*A*mU*G*mC*	3'N-3PS
1193.4300	-5				
2945.0671	-2	5892.1506	5892.1500	mU*mC*A*mC*mU*mU*mU*mC*A*mU*A*A*mU*G*mC	3'N-3
1177.4222	-3				
2788.4119	-2	5578.8394	5578.8400	mU*mC*A*mC*mU*mU*mU*mC*A*mU*A*A*mU*G*	3'N-4PS
1114.7598	-5				
2748.3904	-2	5498.7967	5498.7970	mU*mC*A*mC*mU*mU*mU*mC*A*mU*A*A*mU*G	3'N-4

1098.7513	-5				
2578.7362	-2	5159.4882	5159.4890	mU*mC*A*mC*mU*mU*mU*mC*A*mU*A*A*mU*	3'N-5PS
1030.8896	-5				
2538.7149	-2	5079.4454	5079.4460	mU*mC*A*mC*mU*mU*mU*mC*A*mU*A*A*mU	3'N-5
1014.881	-5				
2381.5677	-2	4765.1515	4765.1520	mU*mC*A*mC*mU*mU*mU*mC*A*mU*A*A*	3'N-6PS
1190.2799	-4				
2341.5462	-2	4685.1086	4685.1090	mU*mC*A*mC*mU*mU*mU*mC*A*mU*A*A	3'N-6
1170.2692	-4				
2179.8924	-2	4361.8008	4361.8000	mU*mC*A*mC*mU*mU*mU*mC*A*mU*A*	3'N-7PS
1089.4422	-4				
2139.871	-2	4281.7572	4281.7570	mU*mC*A*mC*mU*mU*mU*mC*A*mU*A	3'N-7
1069.4311	-4				
1978.2161	-2	3958.4483	3958.4480	mU*mC*A*mC*mU*mU*mU*mC*A*mU*	3'N-8PS
1318.4748	-3				
1938.1941	-2	3878.4048	3878.4050	mU*mC*A*mC*mU*mU*mU*mC*A*mU	3'N-8
1291.7938	-3				
1781.0472	-2	3564.1109	3564.1110	mU*mC*A*mC*mU*mU*mU*mC*A*	3'N-9PS
1187.0291	-3				

1741.0262	-2	3484.0684	3484.0680	mU*mC*A*mC*mU*mU*mU*mC*A	3'N-9
1160.3481	-3				
1579.3714	-2	3160.7587	3160.7590	mU*mC*A*mC*mU*mU*mU*mC*	3'N-10PS
1052.5782	-3				
1539.3503	-2	3080.7163	3080.7160	mU*mC*A*mC*mU*mU*mU*mC	3'N-10
1025.8973	-3				
1382.6951	-2	2767.4062	2767.4060	mU*mC*A*mC*mU*mU*mU*	3'N-11PS
921.4607	-3				
1342.6732	-2	2687.3628	2687.3630	mU*mC*A*mC*mU*mU*mU	3'N-11
894.7797	-3				
1185.5266	-2	2373.0688	2373.0690	mU*mC*A*mC*mU*mU*	3'N-12PS
790.0148	-3				
1145.5054	-2	2293.0264	2293.0260	mU*mC*A*mC*mU*mU	3'N-12
2292.0179	-1				
948.3363	-2	1898.6887	1898.6890	mU*mC*A*mC*mU	3'N-13
1897.6808	-1				
791.1891	-2	1584.3946	1584.3950	mU*mC*A*mC*	3'N-14PS
1583.3869	-1				
1503.3442	-1	1504.3522	1504.3520	mU*mC*A*mC	3'N-14

1190.0341	-1	1191.0421	1191.0420	mU*mC*A*	3'N-15PS
2302.6235	-3	6910.8948	6910.8950	*mC*A*mC*mU*mU*mU*mC*A*mU*A*A*mU*G*mC*mU*G*G	5'N-1PS
1381.1710	-5				
2242.6091	-3	6730.8519	6730.8520	mC*A*mC*mU*mU*mU*mC*A*mU*A*A*mU*G*mC*mU*G*G	5'N-1
1345.1625	-5				
2138.1725	-3	6417.5423	6417.5420	*A*mC*mU*mU*mU*mC*A*mU*A*A*mU*G*mC*mU*G*G	5'N-2PS
1282.5006	-5				
2111.4912	-3	6337.4988	6337.4990	A*mC*mU*mU*mU*mC*A*mU*A*A*mU*G*mC*mU*G*G	5'N-2
1266.492	-5				
2003.7223	-3	6014.1910	6014.1900	*mC*mU*mU*mU*mC*A*mU*A*A*mU*G*mC*mU*G*G	5'N-3PS
1201.8302	-5				
1977.0399	-3	5934.1469	5934.1470	mC*mU*mU*mU*mC*A*mU*A*A*mU*G*mC*mU*G*G	5'N-3
1185.822	-5				
2809.4101	-2	5620.8369	5620.8370	*mU*mU*mU*mC*A*mU*A*A*mU*G*mC*mU*G*G	5'N-4PS
1404.2014	-4				
2769.3892	-2	5540.7942	5540.7940	mU*mU*mU*mC*A*mU*A*A*mU*G*mC*mU*G*G	5'N-4
1384.1905	-4				
2612.2421	-2	5226.5008	5226.5000	*mU*mU*mC*A*mU*A*A*mU*G*mC*mU*G*G	5'N-5PS
1741.1591	-3				

2572.2205	-2	5146.4569	5146.4570	mU*mU*mC*A*mU*A*A*mU*G*mC*mU*G*G	5'N-5
1714.4776	-3				
2415.0732	-2	4832.1630	4832.1630	*mU*mC*A*mU*A*A*mU*G*mC*mU*G*G	5'N-6PS
1207.0329	-4				
2375.0523	-2	4752.1203	4752.1200	mU*mC*A*mU*A*A*mU*G*mC*mU*G*G	5'N-6
1583.032	-3				
2225.904	-2	4453.8248	4453.8250	*mC*A*mU*A*A*mU*G*mC*mU*G*G	5'N-7PS
1483.6005	-3				
2185.8829	-2	4373.7732	4373.7820	mC*A*mU*A*A*mU*G*mC*mU*G*G	5'N-7
1456.9135	-3				
2029.2276	-2	4060.4718	4060.4720	*A*mU*A*A*mU*G*mC*mU*G*G	5'N-8PS
1352.4828	-3				
1989.2063	-2	3980.4289	3980.4290	A*mU*A*A*mU*G*mC*mU*G*G	5'N-8
1325.8017	-3				
1819.5522	-2	3641.1209	3641.1210	*mU*A*A*mU*G*mC*mU*G*G	5'N-9PS
1212.6991	-3				
1779.5308	-2	3561.0777	3561.0780	mU*A*A*mU*G*mC*mU*G*G	5'N-9
1186.0179	-3				

where: * – phosphorothioate group; mU – methyluracil; mC – methylcytosine.